Local Phase Holdups in Gas-Solids Fluidization and Transport

Hsiaotao T. Bi and Peng-Cheng Su
Dept. of Chemical and Biological Engineering, University of British Columbia, Vancouver, BC, V6T 1Z4, Canada

A two-phase structural model consisting of a dense phase and a dilute phase with allowance for the dense-phase expansion and the solids holdup in the dilute phase was developed and successfully applied to the analysis of local voidage fluctuation signals. Such a model can be used to derive local-phase holdups and voidage in each phase in both bubbling/slugging/turbulent fluidized beds and circulating fluidized-bed risers without ambiguity in defining criteria for dividing phases used by previous researchers. Such a model can also explain the existence of a maximum standard deviation at a local voidage around 0.7, and why a maximum peak is observed in the radial profiles of standard deviation of local voidage fluctuations in high-velocity fluidized-bed columns.

Introduction

Local time-averaged solids concentrations in gas–solids fluidization and transport systems can be obtained by several techniques including X-ray, gamma-ray, capacitance probes and optical fiber probes (Yates and Simon, 1994; Louge, 1997). However, only small-size and fast-response capacitance probes, optical fiber probes, and electric sensors are commonly used for the measurement of local instantaneous solids concentrations in gas–solids fluidized beds (Werther, 1999). Compared to capacitance probes, optical fiber probes have a relatively confined measurement volume and are less influenced by changes in the media temperature and moisture content. Therefore, optical fiber probes have been gaining increased application in deducing local instantaneous flow structures in gas–solids fluidized beds. For bubbling and turbulent fluidized-beds, the local bubble/void phase fraction was determined based on a probability distribution of signals obtained within a certain time period. The bubble/void phase fraction can be easily determined if the system is composed of two distinct phases of sharp interface between them. In gas–solids fluidized beds, the dense phase expansion, solids content inside bubbles/voids and the existence of less denser cloud and wake region all make the separation of the two-phase interface difficult. In the open literature, at least five methods have been reported to set a threshold value of the dense phase.

A simple method to separate the dense phase from the dilute phase is to set a threshold in the middle of the difference between the maximum and the minimum value (Bi, 1994), as shown in Figure 1a. For reflection-type optical fiber probes, the amplitude of signals or light intensity received by the receiving fiber is proportional to the solids concentration, and the bubble/void fraction will be equal to the area below the threshold value divided by the total area underneath the probability density function (PDF) curve. The second method argues that the threshold can be set by the minimum point of the PDF curve (Bi, 1994), as shown in Figure 1b. However, it becomes difficult to identify such a minimum point when the PDF curve is very flat in the middle region.

The third method was proposed by Mainland and Welty (1995), who proposed to set a threshold to the point corresponding to 0.05 times the difference between the maximum and the minimum amplitudes, that is, $0.05(V_{max} - V_{min})$ for a light penetration type optical fiber probe. When applied to the reflection-type optical fiber probes, the threshold should be set to $0.95(V_{max} - V_{min})$ (Figure 1c), with the area underneath the curve with amplitude higher than $0.95(V_{max} - V_{min})$ representing the dense phase. The choice of such a threshold appears to be arbitrary, and may not be applicable for other optical fiber systems.

The fourth method was proposed by Yang et al. (1990) based on the assumption that a symmetrical distribution around the peak, corresponding to the dense phase, existed in the PDF curve. Thus, it was proposed to use the area underneath the curve in the region with signal amplitude higher than the dense phase peak multiplied by two, to represent the total area occupied by the dense phase, as shown in Figure 1d.

Wang and Wei (1997) tried to fit the PDF curve with a bimodal distribution function, with one peak corresponding

Correspondence concerning this article should be addressed to H. T. Bi.

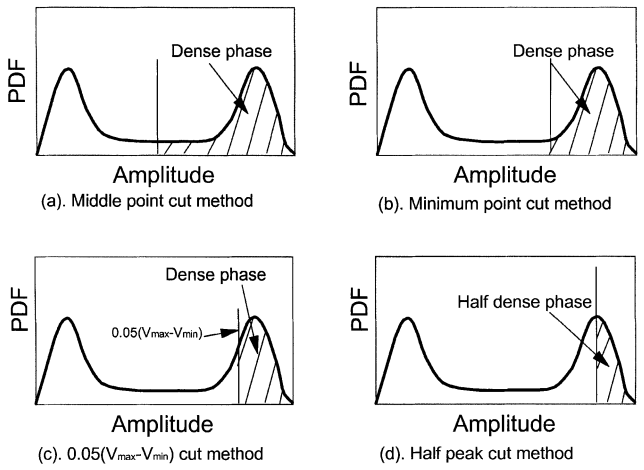

Figure 1. Types of thresholds for separating dense and dilute phases in fluidized beds.

to the dense phase and the other corresponding to the bubble/void phase. It was further assumed that the peak corresponding to the bubble phase follows a log-normal distribution while the peak corresponding to the dense phase follows a normal distribution. The bubble/void phase fraction was then determined by fitting the curve with the bimodal distribution function. Similarly, Cui et al. (2000) fitted their PDF curve with a bimodal distribution function. However, they found that the gamma distribution function gave best agreement with both the dense phase peak and the dilute phase peak for their experimental data.

Although all those methods have been used to give the local bubble/void phase volume fraction in gas–solids fluidized beds, none of them has been experimentally validated. Figure 2 shows the void phase volume fraction estimated using the five methods based on the experimental data of Bi (1994) obtained in a 0.1 m fluidized beds with FCC particles. It is seen that the void phase volume fraction varies significantly

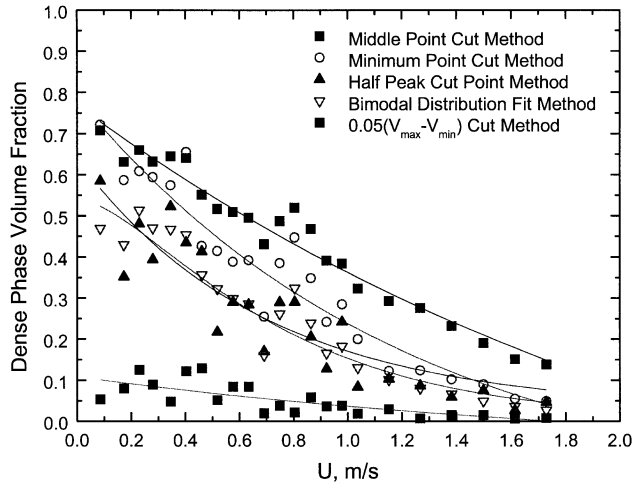

Figure 2. Comparison of local-dilute-phase volume fraction obtained based on different types of thresholds.

when different methods are used. This raises the question concerning how one can compare the void phase volume fraction data obtained from different sources based on different techniques, and how to use these results in the modeling of two-phase bubbling/turbulent fluidized-bed reactors. The present work proposed a simple method based on the two-phase flow theory for the estimation of local phase holdups based on local voidage fluctuation signals.

New Technique Based on a Nonideal Two-Phase Flow Model

Model equations

For two-phase flow with the dense phase voidage of ϵ_d and the dilute/bubble phase voidage equal to ϵ_b, a small optical fiber probe will register signals of ϵ_d and ϵ_b when exposed to the dense and dilute phase, respectively. The local averaged voidage ϵ, the variance/standard deviation (S), skewness (S_k) and flatness (f) of the signals are related to the bubble phase volume fraction δ_b by

$$\epsilon = \delta_b \epsilon_b + (1-\delta_b)\epsilon_d \tag{1}$$

$$S = \sqrt{(\epsilon_b - \epsilon)^2 \delta_b + (\epsilon_d - \epsilon)^2 (1-\delta_b)} \tag{2}$$

$$S_k = \frac{1}{S^3}\left[(\epsilon_b - \epsilon)^2 \delta_b + (\epsilon_d - \epsilon)^3 (1-\delta_b)\right] \tag{3}$$

$$f = \frac{1}{S^4}\left[(\epsilon_b - \epsilon)^4 \delta_b + (\epsilon_d - \epsilon)^4 (1-\delta_b)\right] \tag{4}$$

Figure 3 shows the standard deviation of local voidage fluctuations as a function of local voidage at various values of ϵ_b and ϵ_d. For ideal two-phase flow, the standard deviation reaches a maximum value at $(\epsilon_b + \epsilon_d)/2$. When the dense phase voidage or the dilute phase voidage varies, both the maximum standard deviation and the voidage corresponding to the maximum point will be shifted. Figure 4 shows the skewness of local voidage fluctuations based on Eq. 3. The skewness generally decreases with increasing local voidage and crosses zero at $(\epsilon_b + \epsilon_d)/2$. Again, both the value and the zero crossing point shift with variations of dense phase and dilute phase voidage. For ideal bubbly flow with $\epsilon_d = \epsilon_{mf} = 0.46$ and $\epsilon_b = 1$, the voidage corresponding to the maximum standard deviation and zero skewness value is 0.73.

In gas–solids fluidized beds, the bubble phase is always trapped with a certain amount of particles, while the dense phase may expand with increasing superficial gas velocity. In addition, the boundary between the bubble and the dense phase is quite diffuse due to the existence of a cloud region and a wake region. All these will make the local voidage variations deviate from the ideal bubbly flow as described by Eqs. 1 to 4. Figure 5 shows the standard deviation of local voidage fluctuations from a reflection-type optical fiber probe in a 0.1 m diameter fluidized bed with both FCC and sand particles of 58 and 150 μm, respectively. The details of the experimental setup and measurement can be found from Bi and Grace (1995). It is seen that the calculated standard deviations are generally lower than predicted by the ideal bubbly flow with $\epsilon_d = \epsilon_{mf} = 0.46$ and $\epsilon_b = 1$, and the voidage corresponding to the maximum value is higher than predicted. Comparing FCC

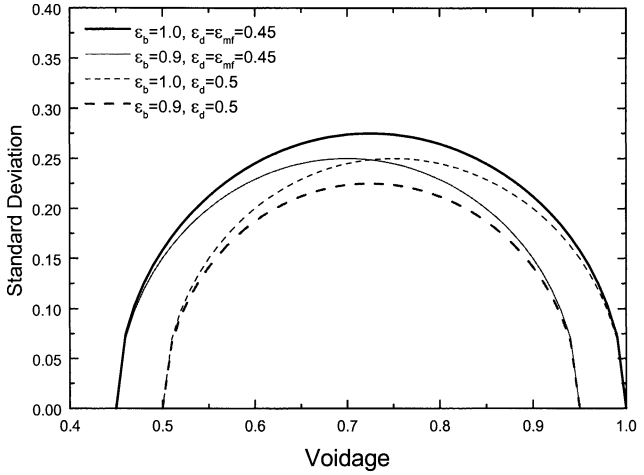

Figure 3. Standard deviations of local voidage fluctuations for ideal and nonideal two-phase flows.

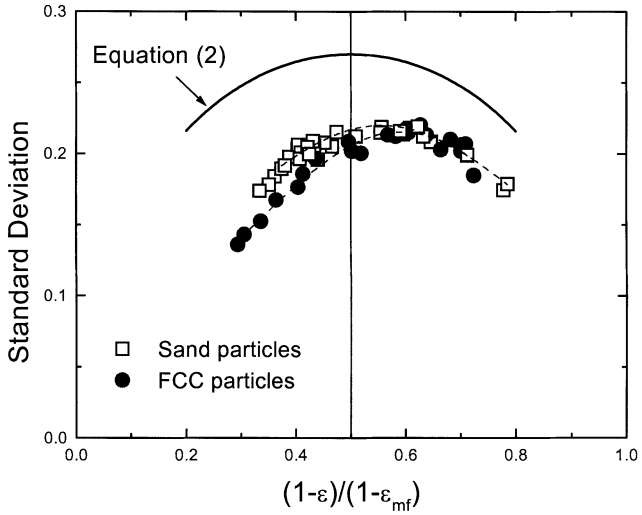

Figure 5. Standard deviation of local voidage fluctuations: model simulation vs. experimental data of Bi (1994).

and sand particles, it is seen that the deviation from the theoretical prediction for ideal two-phase bubbly flow is more significant for FCC particles than sand particles, implying that the bubbly flow with sand particles is closer to the ideal two-phase flow. This is consistent with most observations that there are more solids inside the bubbles and that the dense phase expands more significantly with increasing superficial gas velocity for fine Group A powders.

The skewness and flatness of local voidage fluctuations are presented in Figure 6 for both FCC and sand particles. Both skewness and flatness for both sand and FCC particles are generally higher than predicted from the ideal two-phase flow model. The deviation is more significant for FCC particles than sand particles, indicating that the solids content inside the bubble phase and the dense phase expansion may not be ignored. Especially for FCC particles, the dense phase expansion and solids content inside the bubble phase are important parameters, which need to be included in the interpretation of optical signals.

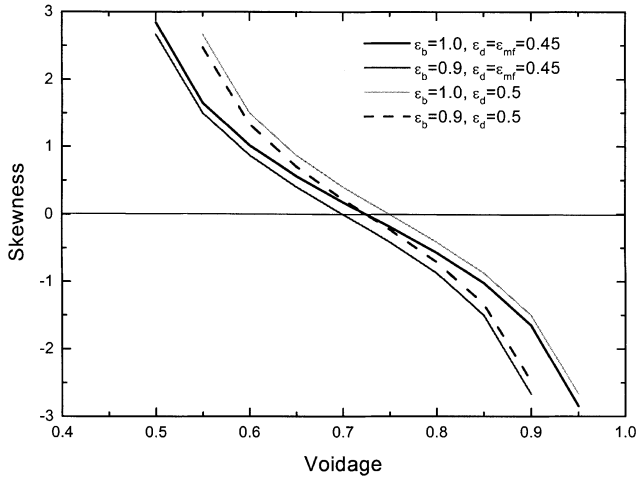

Figure 4. Skewness of local voidage fluctuations for ideal and nonideal two-phase flows.

Parameter estimation for nonideal two-phase flows

To estimate the parameters for nonideal two-phase bubbly flow with allowance for the dense phase expansion and solids holdup in the dilute bubble phase based on local voidage signals, Eqs. 1 to 3 are rearranged to

$$\epsilon_d = \epsilon - \frac{S}{2}\left[\sqrt{4+S_k^2} - S_k\right] \tag{5}$$

$$\epsilon_b = S.S_k + 2\epsilon - \epsilon_d \tag{6}$$

$$\delta_b = (\epsilon - \epsilon_d)/(\epsilon_b - \epsilon_d) \tag{7}$$

With ϵ, S and S_k calculated from local voidage fluctuation signals, the dense phase voidage ϵ_d, dilute phase voidage ϵ_b, and the dilute phase volume fraction δ_b can be estimated from above equations.

Figure 7 shows the calculated values of ϵ_d, ϵ_b and δ_b as a function of the local average voidage based on data obtained at the center and the near wall region of a 0.1 m diameter column for FCC particles. It is seen that the local dilute phase volume fraction increases with increasing the local average voidage. The dense phase voidage is around 0.5 at relatively low voidage and increases with increasing local average voidage at high voidage, indicating that the dense phase remains unchanged at low gas velocities and starts to expand at relatively high velocities when local average voidage exceeds 0.70. This is consistent with experimental observations that the dense phase starts to expand when the flow pattern transforms into the turbulent fluidization (Nakajima et al., 1991; Bi and Grace, 1995). The dilute phase voidage is around 0.9,

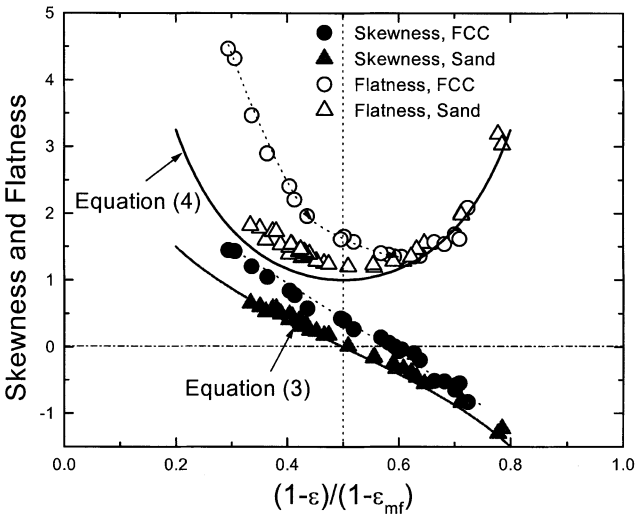

Figure 6. Skewness and flatness of local voidage fluctuations: model simulation vs. experimental data of Bi (1994).

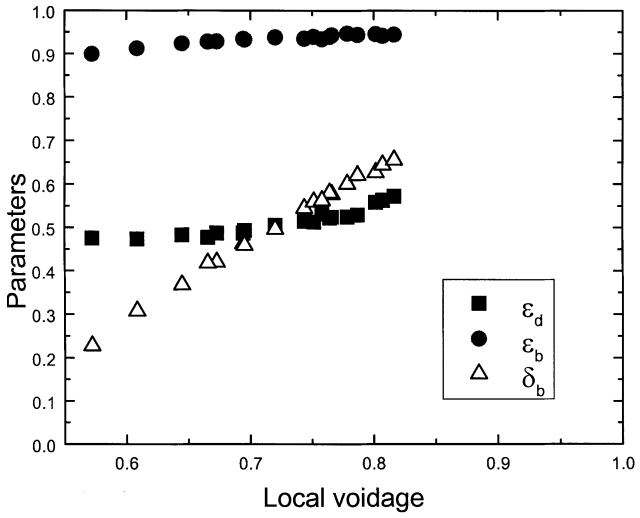

Figure 8. Local dense phase and dilute phase voidages and dilute phase volume fraction in the bubbling/turbulent fluidized bed with sand particles.

Data from Bi, 1994.

much lower than what is expected in gas–solids fluidized beds. It has generally been observed in 2-D beds that the solids content in the bubble phase is between 0.1 to 1%. The dilute phase voidage is thus expected to be around 0.99. Possible causes of such high solid content in the bubble phase include the variation of the voidage around the bubble boundary due to the existence of the cloud and the wake, and the distortion of bubbles due to the interaction between bubbles and the probe. Figure 7 also shows that there is only slight difference between the central region and the near wall region in the column. At the axis, the dense phase voidage is slightly lower than at $r/R = 0.8$, while the dilute phase voidage is essentially the same at both regions. Due to the lower expansion of the dense phase at the axis, the dilute phase volume fraction at the axis is slightly higher than at $r/R = 0.8$.

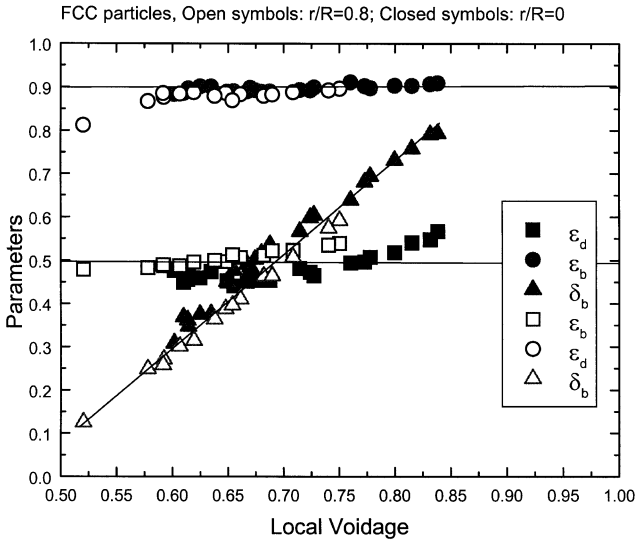

Figure 7. Local-dense-phase and dilute-phase voidages and dilute phase volume fraction in the bubbling/turbulent fluidized bed with FCC particles.

Data from Bi, 1994.

Results for sand particles are shown in Figure 8. The dilute phase voidage is seen to be higher than FCC particles, indicating less solids content in the bubble phase with sand particles. The dense phase voidage remains at around 0.48 at ϵ less than 0.7, and starts to increase afterward. Compared to FCC particles, the dense phase voidage is slightly lower for sand particles. The dilute phase volume fraction increases almost linearly with increasing local mean voidage, and is generally lower than the FCC particles. This suggests that the bubble phase volume fraction is higher for FCC particles than sand particles, likely due to the smaller bubble size and the lower bubble rise velocity in the bed with FCC particles.

Discussions

Comparison with other methods

As shown in Figure 2, the void phase volume fraction varies with the method. The method proposed in this work divides signals directly into two phases with allowance for the expansion in the dense phase and solids content in the bubble phase. Therefore, the parameters estimated in such a way can be directly used in the two-phase reactor models. Such a method also avoids the arbitrary selection of the threshold for the division of the two phases from the probability distribution curve (such as the minimum point, 5% amplitude, and the peak point) or the selection of the proper distribution functions for both peaks in the probability distribution curve (such as normal, log-normal and gamma function).

Maximum standard deviation of local voidage fluctuations and dense phase expansion

Both the model and experimental data show that the standard deviation of local voidage fluctuations reaches a maxi-

mum value at a local mean voidage around 0.7 when the probe is equally exposed to the bubble phase and the dense phase. Such a point demarcates the phase inversion, with bubble phase fraction overweighing the dense phase beyond this point, and is not necessarily related to the change of bubble sizes or shapes. Therefore, it does not necessarily correspond to the transition from bubbling to turbulent fluidization if such a transition is believed to occur when bubble breakup overtakes bubble coalescence (Cai et al., 1990). As shown in Figure 5, the standard deviation of local voidage fluctuations reaches a maximum at approximately the same local mean voidage for both FCC and sand particles, although the flow pattern for sand particles may transform from slugging to intermittent flow, while a transformation from bubbling to turbulent fluidization occurs for FCC particles (Bi et al., 1995a).

Figures 7 and 8 show that the local dense phase voidage remains almost constant when the local mean voidage is below 0.7, and starts to expand after ϵ exceeds 0.7 to 0.75. Similar results were reported by Nakajima et al. (1991) using fine catalyst particles, and the point at which the dense phase starts to expand was claimed to correspond to the transition from bubbling to turbulent fluidization. The present analysis shows that such a transition point coincides with the point when the local dense phase and dilute phase holdups become approximately equal. Therefore, the expansion of the dense phase may be triggered by the phase inversion when the dilute phase fraction surpasses the dense phase fraction. The triggering mechanism seems to be in agreement with the speculation (Bi et al., 1995a) that bubbles become highly unstable when they are closely packed in the fluidized bed due to the strong interaction of bubble roof with the turbulent wake of the leading bubble. The splitting of large bubbles consequently agitates the dense phase and leads to the expansion of the dense phase.

Radial profiles of the standard deviation of local voidage fluctuations and the core-annulus boundary

In CFB risers operated in the turbulent and fast fluidization regimes, it has been reported that there exists a maximum point on the radial profiles of the standard deviation and intermittency index of local voidage fluctuations (Brereton and Grace, 1993; Bai et al., 1999; Issangya et al., 2000). Such a maximum point has been speculated to correspond to the boundary between the dilute core region and the dense annulus region in which net particle flow is downward, although the wall layer thickness defined by this maximum point was found to be quite larger than the one obtained from local solids flux measurement (Issangya et al., 2000).

Figure 9a shows typical radial profiles of standard deviation of local voidage fluctuations for radial voidage profiles in Figure 9b. The radial voidage profile for each given cross-sectional averaged voidage is calculated by the Zhang et al. (1991) correlation

$$\epsilon = \bar{\epsilon}^{\,0.19 + (r/R)^{2.5} + 3(r/R)^{11}} \tag{7}$$

A dense phase voidage of 0.45 and a dilute phase voidage of 1.0 are used in the simulation.

It is seen that a peak is identified on the radial profiles of standard deviation of local voidage fluctuations when the radial voidage profile crosses with $\epsilon = 0.725$. The peak thus corresponds to the point where the dense phase volume fraction is equal to the dilute phase volume fraction. The boundary between the core and the annulus in the riser is commonly defined by the point where net solids flux changes from upward to downward. The peak point identified in Figure 9 does not necessarily correspond to such a change in particle flow direction, and, therefore, the peak point could not be used to determine the core-annulus boundary.

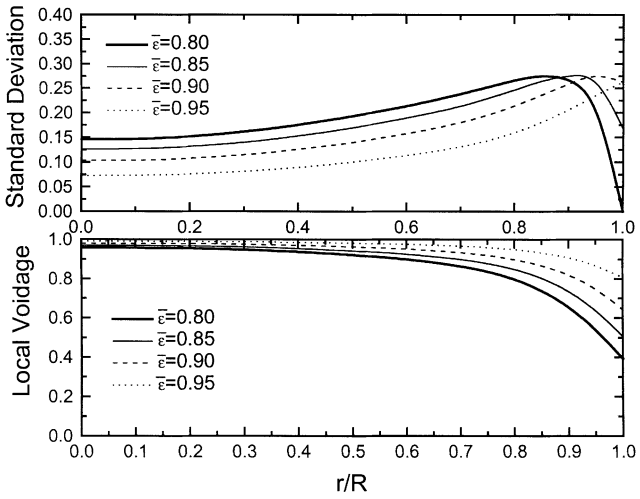

Figure 9. Simulated radial profiles of standard deviation of local voidage fluctuations in CFB risers.

Two-phase flow structure in the near wall region of the riser

The particle flow in the near wall region in a CFB riser is composed of a dispersed dilute phase and a dense cluster/streamer phase. Such a two-phase flow structure has been measured using both capacitance probes (Brereton and Grace, 1993) and optical fiber probes (Zhang et al., 1991). To extract the information on phase holdup and solids contents in both dispersed phase and the cluster/streamer phase, Eqs. 5 to 7 can be applied. Figure 10 shows the estimated dispersed phase volume fraction and the voidage in both the dispersed phase and the cluster phase based on signals from an optical fiber probe located near the inner riser wall of a 0.15×0.15 m^2 square column. The same sand particles are used as in the experiment presented in Figure 8 with a mean diameter of 215 μm. Experimental details can be found in Bi et al. (1995b). It can be seen that the dilute phase volume fraction decreases with decreasing local voidage, and approaches zero at local voidage around 0.7, indicating that the wall region will be fully covered by the dense phase at such a low local voidage. The dense phase voidage is seen to decrease with decreasing the local voidage and become stabilized at a value around 0.7, much higher than the voidage at minimum fluidization (around 0.4 for sand particles). This suggests that the cluster/streamer phase is highly aerated in the high-velocity circulating fluidized-bed riser. The dilute phase voidage is not so sensitive to the local voidage.

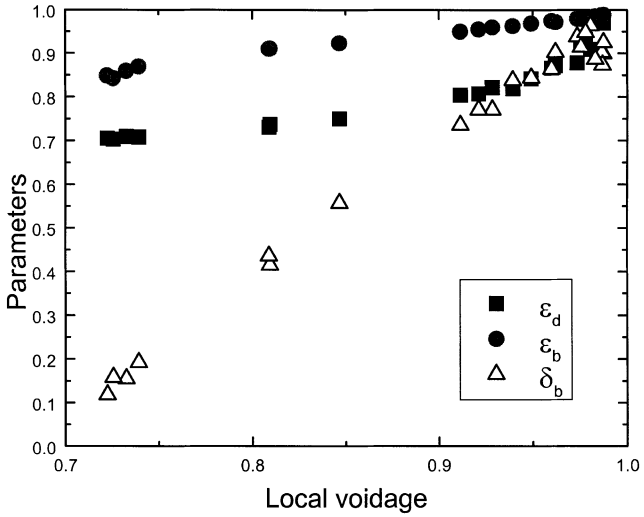

Figure 10. Dense-and dilute-phase voidage and dilute phase volume fraction as a function of local voidage near the wall region of a CFB riser with sand particles.

Data from Bi (1994).

Figure 11 compares the skewness of local voidage signals from the low velocity bubbling/slugging/turbulent fluidized bed and from the high velocity circulating fluidized bed using the same sand particles. It is seen that the skewness from the CFB riser is much lower than from the bubbling/slugging/turbulent bed, with the latter agreeing well with the ideal two-phase flow model. Such a deviation is consistent with the low dilute phase volume fraction and high voidage in the cluster/streamer phase observed in Figure 10.

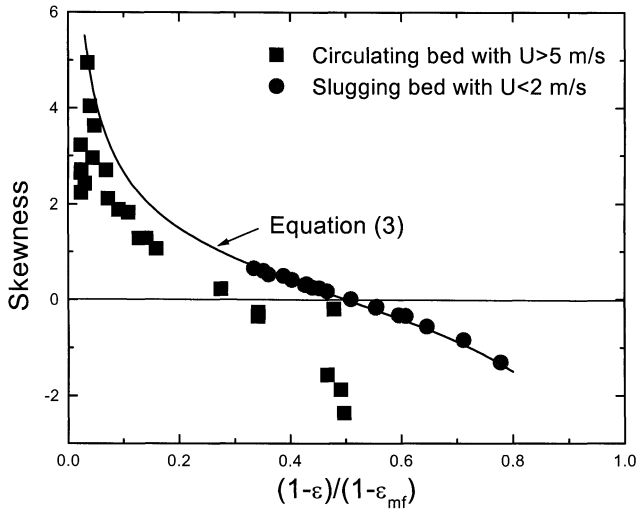

Figure 11. Skewness in the near wall region of a bubbling/turbulent fluidized bed and a CFB riser with sand particles.

Data from Bi (1994).

Conclusions

The local voidage fluctuation signals are analyzed based on a two-phase structural model, which considers the existence of a dense phase and a dilute phase with allowance for the dense phase expansion and the solids holdup in the dilute phase. Based on the analysis of experimental data obtained in a bubbling/turbulent fluidized-bed column with FCC and sand particles, it is demonstrated that such a model can be used to derive local phase holdups and voidage in each phase in both bubbling/slugging/turbulent fluidized beds. Meanwhile, such an approach avoids the ambiguity in defining criteria for dividing phases used by previous researchers. Such a model further predicts the existence of a maximum standard deviation at a local voidage around 0.7, and provides an explanation on why a maximum peak is observed in the radial profiles of standard deviation of local voidage fluctuations in high velocity fluidized-bed columns.

Acknowledgment

The authors are grateful to the Natural Sciences and Engineering Research Council of Canada for supporting this work.

Notation

f = flatness of local voidage fluctuations
r = radial position, m
R = radius of the column, m
S = standard deviation of local voidage fluctuations
S_k = skewness of local voidage fluctuations
V_{max} = maximum signal output, V
V_{min} = minimum signal output, V
δ_b = volume fraction of bubble/dilute phase
ϵ = local average voidage
$\bar{\epsilon}$ = cross-sectional average voidage
ϵ_b = voidage in the bubble/dilute phase
ϵ_d = voidage in the dense phase

Literature Cited

Bai, D. R., A. S. Issangya, and J. R. Grace, "Characteristics of Gas Fluidized Beds in Different Flow Regimes," *Ind. Eng. Chem. Res.*, **38**, 803 (1999).

Bi, H. T., *Flow Regime Transitions of Gas-Solid Fluidization and Transport,* PhD Thesis, University of British Columbia, Vancouver, BC, Canada (1994).

Bi, H. T., and J. R. Grace, "Effects of Measurements on Transition Velocities Used to Demarcate the Onset of Turbulent Fluidization," *Chem. Eng. J.*, **57**, 261 (1995).

Bi, H. T., J. R. Grace, and K. S. Lim, "Mechanism of Transition from Bubbling to Turbulent Fluidization," *Ind. Eng. Chem. Res. Dev.*, **34**, 4003 (1995a).

Bi, H. T., J. R. Grace, and J. X. Zhu, "Transition Velocities Affecting Regime Transitions in Gas-Solids Suspensions and Fluidized Beds," *Chem. Eng. Res. Des.*, **73A**, 163 (1995b).

Brereton, C. M. H., and J. R. Grace, "Microstructural Aspects of the Behaviour of Circulating Fluidized Beds," *Chem. Eng. Sci.*, **48**, 2565 (1993).

Cai, P., Y. Jin, Z. Q. Yu, and Z. W. Wang, "Mechanism of Flow Regime Transition from Bubbling to Turbulent Fluidization," *AIChE J.*, **36**, 955 (1990).

Cui, H., N. Mostoufi, and J. Chaouki, "Characterization of Dynamic Gas-Solid Distribution in Fluidized Beds," *Chem. Eng. J.*, **79**, 133 (2000).

Issangya, A. S., J. R. Grace, D. R. Bai, and J. X. Zhu, "Further Measurement of Flow Dynamics in a High-Density Circulating

Fluidized Bed Riser," *Powder Technol.*, **111**, 104 (2000).
Louge, M., "Experimental Techniques," *Circulating Fluidized Beds*, Chapter, 9, J. R. Grace, A. A. Avidan and T. M. Knowlton eds., Chapman & Hall, London, p. 312 (1997).
Mainland, M. E., and J. R. Welty, "Use of Optical Probes to Characterize Bubble Behavior in Gas-Solid Fluidized Beds," *AIChE J.*, **41**, 223 (1995).
Nakajima, M., M. Harada, M. Asai, R. Yamazaki, and G. Jimbo, "Bubble Fraction and Voidage in an Emulsion Phase in the Transition to a Turbulent Fluidized Bed," *Circulating Fluidized Bed Technology III*, P. Basu, M. Horio and M. Hasatani, eds., Pergamon Press, Oxford, p. 79 (1991).
Wang, Z., and F. Wei, "Similar Distribution Profiles of Local Solids Holdup in Bubbling and Turbulent Fluidized Beds," *Proc. Chinese Particuology Soc. Meeting*, Y. Jin, Z. Q. Yu, and H. Li, eds., Tsinghua University Press, Beijing, China, p. 396 (1997).
Werther, J., "Measurement Techniques in Fluidized Beds," *Powder Technol.*, **102**, 15 (1999).
Yang, Y. R., S. X. Rong, G. Chen, and B. C. Chen, "Flow Regimes and Regime Transitions in Turbulent Fluidized Beds," *Chem. Reaction Eng. and Technol.* (in Chinese), **6**, 9 (1990).
Yates, J. G., and S. J. R. Simons, "Experimental Methods in Fluidization Research," *Int. J. Multiphase Flow*, **20**, supplement, 297 (1994).
Zhang, W., Y. Tung, and F. Johnsson, "Radial Voidage Profiles in Fast Fluidized Bed of Different Diameters," *Chem. Eng. Sci.*, **46**, 3045 (1991).

Manuscript received Oct. 25, 2000, and revision received Mar. 20, 2001.